

Instability of planar vortices in two-dimensional easy-plane Heisenberg model with distance-dependent interactions

Myoung Won Cho* and Seunghwan Kim†

Asia Pacific Center for Theoretical Physics & NCSL, Department of Physics,
Pohang University of Science and Technology, Kyungpook, Pohang, 790-784, South Korea
(Dated: November 18, 2018)

It is known that magnetic vortices in two dimensional Heisenberg models with easy-plane anisotropy exhibit an instability depending on the anisotropy strength. In this paper, we study the statistic behavior of the two-dimensional easy-plane Heisenberg models with distance-dependent interactions, $J_{xy}(r)$ and $J_z(r)$ for in-plane and out-of-plane components. We develop analytical and numerical methods for accurate determination of critical anisotropy, above which out-of-plane vortices are stable. In particular, we explore the vortex formation of the Gaussian-type interaction model and determine the critical anisotropy accurately for square, hexagonal and triangular lattices.

I. INTRODUCTION

The magnetism in two-dimension has been the subject of continued interest in the last few decades, which is aroused further due to recent additions of new materials such as Cu-based high-temperature superconductors and advances in both numerical and experimental capabilities. The classical two-dimensional anisotropic Heisenberg model (CTDAHM) with the spin Hamiltonian,

$$H = -K \sum_{\langle i,j \rangle} (S_i^x S_j^x + S_i^y S_j^y + \lambda S_i^z S_j^z) \quad (1.1)$$

for a coupling constant K , has been one of the most studied models for magnetic systems. For $\lambda = 0$, it becomes the so-called XY model, which is well understood following the work of Berezinskii¹ and Kosterlitz and Thouless². It has a phase transition at T_{KT} , named the Kosterlitz-Thouless phase transition, which can be characterized by a vortex-antivortex unbinding³. For $\lambda < 1$, it belongs to the universality class of the XY model, and it has been known that there are two different types of nonlinear solutions, called “in-plane” and “out-of-plane” vortices⁴. There have been several attempts with numerical simulations and analytic calculations to obtain the critical anisotropy λ_c , above which the out-of-plane vortices are stabilized. At first, Gouvêa *et al.*⁵ investigated the development of the out-of-plane vortex by using a combined Monte Carlo-molecular-dynamics technique. They found that initial out-of-plane vortex relaxes to a planar one below the critical anisotropy $\lambda \approx 0.72$, 0.86, 0.62 for square, hexagonal and triangular lattices respectively. Costa and Costa⁶ obtained a more precise measurement $\lambda_c \approx 0.709$ for a square lattice by fitting the out-of-plane squared component $(S_z)^2$ at the central peak as a function of λ . Wysin made an analysis of the core region of a vortex on a discrete lattice and obtained an estimate of $\lambda_c \approx 0.7044$ for the square lattice⁷, which is improved further to a very accurate value of $\lambda_c \approx 0.703409$ by iteratively setting each spin’s xy components to point along the direction of the effective field due to its neighbors.

Recently, we showed that the pattern formation in pri-

mary visual cortex is also related with the vortex dynamics in magnetism⁸. It is observed *in vivo* that the development of strong scalar components (ocular dominance column) near the singularity centers at orientational components (orientation column). There are at least three different types in observed ocular dominance patterns *in vivo*, which correspond to the Ising type, stable out-of-plane vortex, and stable in-plane vortex behaviors⁹. The determination of the critical anisotropy is important in describing the region of different behaviors in vortex patterns.

In this paper, we consider the two-dimensional easy-plane (XY) symmetry Heisenberg model with distance-dependent interactions :

$$H = - \sum_{i,j} \{ J_{xy}(r_{ij})(S_i^x S_j^x + S_i^y S_j^y) + J_z(r_{ij}) S_i^z S_j^z \} \quad (1.2)$$

for the classical spin variables $\mathbf{S}_i = (S_i^x, S_i^y, S_i^z)$ and the distance dependent exchange energy $J_\mu(r) = \varepsilon_\mu I_\mu(r)/2$ ($\mu = xy$ or z). The dimensionless neighborhood interaction function $I_\mu(r)$ can have a various shape but is expected to be a smooth function and approach zero as $r \rightarrow \infty$. Comparing Eq.(1.2) with Eq.(1.1), we may expect that the anisotropy in the strength of interactions between in-plane and out-of-plane components is $\lambda \sim J_z/J_{xy}$ and obviously $\lambda = \varepsilon_z/\varepsilon_{xy}$ if $I_{xy}(r) = I_z(r)$ for all r . But a more clear definition of the anisotropy parameter λ will be needed for the case of arbitrary interaction functions with $I_{xy}(r) \neq I_z(r)$. Takeno and Homma showed that the anisotropic Heisenberg model with distance-dependent interactions has two different minima in H depending on the ground-state energy of in-plane and out-of-plane components¹⁰. We determine the anisotropy λ by the ratio of the ground-state energy, which is the boundary of the crossover behavior between the XY and Ising models. The critical anisotropy now may depend on the shape and parameter values of $J_\mu(r)$.

In Sec. II, we build an effective Hamiltonian in a continuum approximation for the arbitrary exchange energy function $J(r)$. The continuum theory helps to predict or understand the major behavior of spin configurations and vortex formation. But the exact estimation of the

critical anisotropy cannot be obtained by a continuum approximation because of the singularity near the vortex core⁷. Sometimes two distinct spin models can yield the same Hamiltonian in a continuum approximation. We will show that different values of the critical anisotropy λ_c is possible in spite of the common approximated Hamiltonian (Sec. V). In Sec. III, we generalize and extend Wysin's method^{7,11}, which is the analytic method for obtaining the exact critical anisotropy λ_c in the distant neighbor interaction models. We clarify our method by calculating critical anisotropies of the CTDAHM with $I(r) = \delta(r - 1)$ for different lattice types and comparing them to values. In Sec. IV, we exhibit a simulation method for the determination of the critical value of anisotropy above which out-of-plane components develop. We find that the out-of-plane components start to develop for $\lambda \geq \lambda_c$ where λ_c are 0.7035, 0.8330 and 0.6129 in four-digit accuracy for square, hexagonal and triangular lattices, respectively. These values from simulations are the closest values to the analytic calculations¹¹. In Sec. V, we investigate the critical anisotropy in the two-dimensional easy-plane Heisenberg model with Gaussian type interactions of $I_\mu(r) = \exp(-r^2/2\sigma_\mu^2)$ and the anisotropy $\lambda = (\varepsilon_z/\varepsilon_{xy})(\sigma_z^2/\sigma_{xy}^2)$. We obtain the critical anisotropy λ_c for $\lambda = \varepsilon_z/\varepsilon_{xy}$ ($\sigma_{xy} = \sigma_z$) and $\lambda = \sigma_z^2/\sigma_{xy}^2$ ($\varepsilon_{xy} = \varepsilon_z$) depending on the interaction ranges σ_μ for different lattice types and find a general behavior of λ_c .

II. EFFECTIVE HAMILTONIAN APPROACH

The classical spin vector, $S_i = (S_i^x, S_i^y, S_i^z)$, can be specified by two angles of rotation ϕ_i and θ_i ,

$$\mathbf{S}_i = S(\sin \theta_i \cos \phi_i, \sin \theta_i \sin \phi_i, \cos \theta_i). \quad (2.1)$$

In the momentum space representation, we write

$$\tilde{S}_{\mathbf{q}} = \frac{1}{\sqrt{N}} \sum_i S_i e^{-i\mathbf{q}\cdot\mathbf{r}_i}, \quad (2.2)$$

where the vectors \mathbf{q} are restricted to the first Brillouin zone of the simple cubic d -dimensional lattice. Substituting Eqs.(2.1) and (2.2) into the Hamiltonian in Eq.(1.2), we get

$$H = - \sum_{\mathbf{q}} \left\{ \tilde{J}_{xy}(\mathbf{q})(\tilde{S}_{q_x}\tilde{S}_{-q_x} + \tilde{S}_{q_y}\tilde{S}_{-q_y}) + \tilde{J}_z(\mathbf{q})\tilde{S}_{q_z}\tilde{S}_{-q_z} \right\} \quad (2.3)$$

where

$$\tilde{J}_\mu(\mathbf{q}) = \sum_{\mathbf{r}} J_\mu(\mathbf{r})e^{-i\mathbf{q}\cdot\mathbf{r}} \quad (2.4)$$

for $\mu = xy$ or z . If $\tilde{J}_\mu(q)$ has a maximum point at $q = 0$, the approximated Hamiltonian is obtained by the inverse

fourier transform of the expansion in Eq.(2.3) :

$$H \simeq -NJ_s S^2 + \frac{J_s S^2}{4} \int d^2r \left\{ \alpha(1 - m^2)(\nabla\phi)^2 + \alpha[1 - \delta'(1 - m^2)] \frac{(\nabla m)^2}{(1 - m^2)} + 4\delta m^2 \right\} \quad (2.5)$$

where $J_s = \tilde{J}_{xy}(0)$, $J_p = -\tilde{J}_{xy}''(0)/a^2$, $\delta = 1 - \tilde{J}_z(0)/\tilde{J}_{xy}(0)$, $\delta' = 1 - \tilde{J}_z''(0)/\tilde{J}_{xy}''(0)$, $\alpha = 2J_p/J_s$ and $m(\mathbf{r}) = S_z(\mathbf{r})/S$ for the nearest-neighbor distance a . The exchange energy $J_\mu(r)$ need not be fully positive, however, in ferromagnetic behavior systems. Comparing with the approximated Hamiltonian of the CTDAHM in continuum theory⁵, we expect a ferromagnetic behavior if J_s and J_p are positive. The anisotropy λ is described as

$$\lambda = 1 - \delta = J_z(0)/J_{xy}(0), \quad (2.6)$$

which is the ratio of the ground-state energy for in-plane and out-of-plane components. Eq.(2.5) has two different solutions depending on the anisotropy in λ . The total ground-state energy in Eq.(2.5), $\langle H \rangle_0$, is given by $-N\tilde{J}_{xy}(0)S^2$ (or $-N\tilde{J}_z(0)S^2$) and $m^2(\mathbf{r}) = 0$ (or $m^2(\mathbf{r}) = 1$) for all \mathbf{r} when $\lambda < 1$ (or $\lambda > 1$), which is the XY (or Ising)-like solution as shown by Takeno *et al.*¹⁰ The anisotropy satisfies $\lambda = \varepsilon_z/\varepsilon_{xy}$ if $I_{xy}(r) = I_z(r)$ for all r . However $I_{xy}(r) \neq I_z(r)$, the anisotropy can be expressed as $\lambda \propto (\sigma_z/\sigma_{xy})^d$ for the interaction range σ_μ in the d -dimensional lattice because the exchange energy is proportional to the number of interaction pairs in ferromagnetic systems.

III. ANALYTIC CALCULATIONS OF CRITICAL ANISOTROPY

The Hamiltonian in Eq.(1.2), can be rewritten as

$$H = - \sum_{i,j} \{ J_{xy}(\mathbf{r}_{ij}) \sqrt{1 - m_i^2} \sqrt{1 - m_j^2} \cos(\phi_i - \phi_j) + J_z(\mathbf{r}_{ij}) m_i m_j \}, \quad (3.1)$$

where $\phi_i = \tan^{-1}(S_i^y/S_i^x)$ and $m_i = S_i^z/S$. For arbitrary $|m_i| \ll 1$, we get

$$\frac{\partial H}{\partial m_i} \simeq 2 \sum_j \{ J_{xy}(\mathbf{r}_{ij}) m_i \cos(\phi_i - \phi_j) - J_z(\mathbf{r}_{ij}) m_j \} = 0. \quad (3.2)$$

This always has an in-plane vortex solution, $m_i = 0$ for all sites i . For the out-of-plane solutions, which have non-zero m_i components, the determinant of the matrix W should vanish, where

$$W_{\alpha\beta} = \delta_{\alpha\beta} \sum_{i \in M_\alpha} \sum_j J_{xy}(\mathbf{r}_{ij}) \cos(\phi_i - \phi_j) - \sum_{i \in M_\alpha} \sum_{j \in M_\beta} J_z(\mathbf{r}_{ij}). \quad (3.3)$$

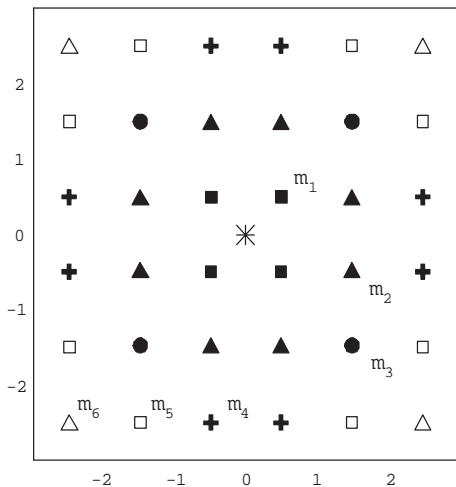


FIG. 1: The vortex center is located at $(0,0)$ and the sites are presented by different symbols according to the distance from the vortex center. (solid squares for $r = 1/\sqrt{2}$, solid triangles for $r = \sqrt{10}/2$, etc.)

For an arbitrary exchange energy function $J_\mu(r)$, $\mu = xy$ or z , the critical value of the anisotropy can be determined by a root finding method for $\det|W(\lambda)| = 0$. When $I_{xy}(r) = I_z(r)$ for all r , so $\lambda = \varepsilon_z/\varepsilon_{xy}$, the boundary for the existence of the out-of-plane solutions can be obtained from the eigenvalue problem,

$$A_\alpha m_\alpha - \lambda w_{\alpha\beta} m_\beta = 0 \quad (3.4)$$

or

$$(w_{\alpha\beta}/A_\alpha)m_\beta = (1/\lambda)m_\alpha \quad (3.5)$$

for

$$A_\alpha = \frac{1}{|M_\alpha|} \sum_{i \in M_\alpha} \sum_j I(\mathbf{r}_{ij}) \cos(\phi_i - \phi_j) \quad (3.6)$$

and

$$w_{\alpha\beta} = \frac{1}{|M_\alpha|} \sum_{i \in M_\alpha} \sum_{j \in M_\beta} I(\mathbf{r}_{ij}) \quad (3.7)$$

where α or β is a block index rather than a site index when there exists a symmetry in the lattice geometry and $M_\alpha = \{i \mid r_i = r_\alpha\}$ are sets ordered by the distance from the vortex core ($1 \leq \alpha \leq L$). The maximum eigenvalue, which is equal to $1/\lambda_c$, is determined by using only the nearest components to the core center, $m_1, m_2, \dots, m_{\mathcal{N}}$ ($1 \leq \mathcal{N} \leq L$, where \mathcal{N} is the number of the nearest components).

Note that we assume that the center of the vortex is located at the origin of a coordinate system. The in-plane angles are chosen to be the usual solution of the in-plane vortex in the continuum theory, $\phi_i = \tan^{-1}(y_i/x_i)$, or

$$\cos(\phi_i - \phi_j) = \hat{\mathbf{r}}_i \cdot \hat{\mathbf{r}}_j. \quad (3.8)$$

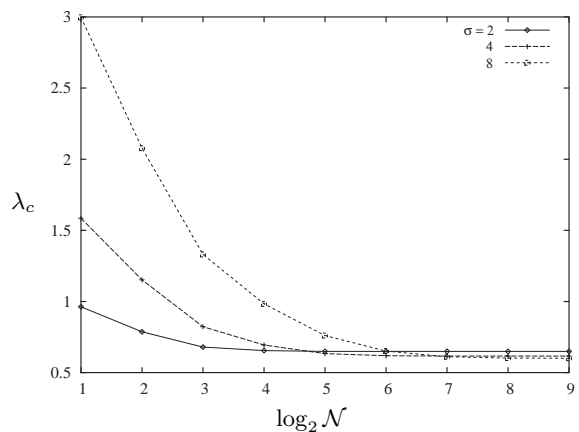


FIG. 2: The critical anisotropy λ_c as a function of $\log_2 \mathcal{N}$ for the anisotropic Heisenberg model with Gaussian type interactions for $\sigma = 2, 4$ and 8 . As σ increases, the size of the out-of-plane vortex core increases.

For the CTDAHM in Eq.(1.1), the interaction function is given by $I(\mathbf{r}) = \delta(r - 1)$ and

$$\begin{aligned} A_1 &= \frac{4}{\sqrt{5}} \\ A_2 &= \frac{4}{\sqrt{5}} \left(1 + \frac{1}{\sqrt{5}} + \frac{2}{\sqrt{13}}\right) \\ w_{11} &= w_{12} = 2 \\ w_{21} &= w_{22} = 1, \end{aligned} \quad (3.9)$$

where $M_1 = \{\pm(1/2, 1/2), \pm(1/2, -1/2)\}$ and $M_2 = \{\pm(3/2, 1/2), \pm(3/2, -1/2), \pm(1/2, 3/2), \pm(1/2, -3/2)\}$ for the square lattice in Fig 1. In this case, $w_{\alpha\beta}$ is just the number of the nearest neighbors that belong to the set M_β for $m_i \in M_\alpha$. The critical anisotropy, where the 2×2 determinant vanishes, is given by

$$\lambda_c = \frac{A_1 A_2}{A_1 + 2A_2} \approx 0.7157 \quad (3.10)$$

which agrees well with the results of Wysin⁷. Wysin also showed the λ_c is determined by the zero of a 3×3 determinant as 0.7044. We obtain a smaller critical value of $\lambda_c \approx 0.6974$ for $\mathcal{N} = 4$, which converges to 0.6941 in four-digit accuracy for $\mathcal{N} \geq 16$. This critical value show a deviation from the result in numerical simulations. Wysin showed that there are some differences in the discrete solution from the continuum results especially near the vortex core¹¹. Similar to Wysin's process, we eliminate this difference between discrete and continuum solutions by evolution of each spin's xy components to point along the direction of the effective field due to its neighbors, and we obtain $\lambda_c \approx 0.703420$, which is very close to the value obtained by Wysin's, $\lambda_c \approx 0.703409$, and one from our simulations in Sec. IV ($\lambda_c \approx 0.7035$).

For the nearest-neighbor interactions in the CTDAHM, the size of the vortex core is small, which leads to precise determination of the critical anisotropy for relatively small \mathcal{N} . But as the interaction range increases,

the size of the vortex core increases and more components of the matrix are needed to obtain the accurate value of λ_c . Fig. 2 shows the computed anisotropy λ_c as a function of \mathcal{N} for different interaction ranges σ_μ in Gaussian type interactions. The convergence of different lines for different ranges gives an estimate of the vortex core size r_v . For the average number of the degeneracy g per block M_α , $g\mathcal{N}_c$ means the number of spin sites which contributes to the determination of λ_c . The radius of the vortex core can be estimated as

$$r_v \sim \sqrt{\frac{g}{\pi} \mathcal{N}_c} \quad (3.11)$$

with g approaching 8 for large \mathcal{N}_c for the square lattice or the D_4 symmetry geometry.

IV. SINGLE-VORTEX SIMULATIONS

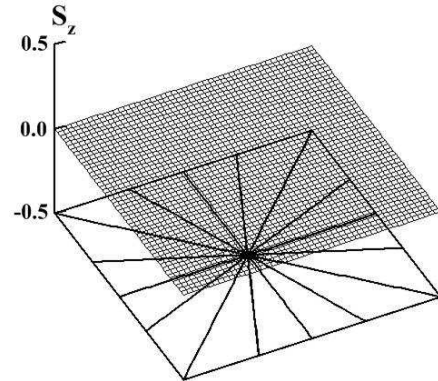
In general, it is quite difficult to determine the critical anisotropy precisely with a simulated annealing approach using Monte Carlo simulations. In particular, for the distance-dependent interaction models, the longer annealing time is required due to the larger lattice size and the larger cutoff range. Our numerical simulations are carried out by evolving dynamical equations as a gradient flow, which allows a more accurate determination of the vortex behavior near $\lambda \sim \lambda_c$. The discrete equations of motion used in simulations are

$$\begin{aligned} \frac{\partial \phi_i}{\partial t} &= -\frac{\partial H}{\partial \phi_i} \\ &= -2 \sum_j J_{xy}(r_{ij}) \sin \theta_i \sin \theta_j \sin(\phi_i - \phi_j) \end{aligned} \quad (4.1a)$$

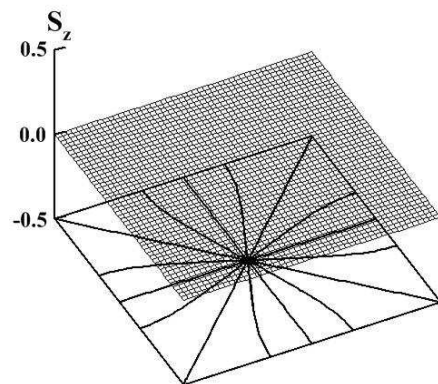
$$\begin{aligned} \frac{\partial \theta_i}{\partial t} &= -\frac{\partial H}{\partial \theta_i} \\ &= 2 \sum_j \{ J_{xy}(r_{ij}) \cos \theta_i \sin \theta_j \cos(\phi_i - \phi_j) \\ &\quad - J_z(r_{ij}) \sin \theta_i \cos \theta_j \} \end{aligned} \quad (4.1b)$$

at zero temperature. The simulations start from an initial state of a planar vortex on the lattice center and small random fluctuations in out-of-plane components ($|S_z| < 10^{-6}$).

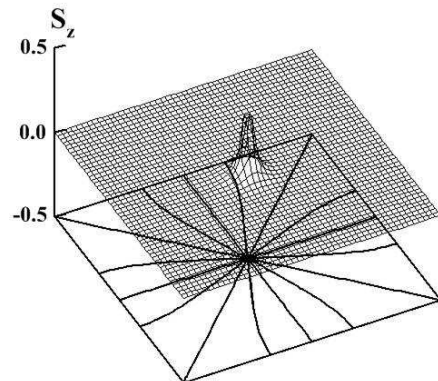
A problem in the single vortex simulations is the effect of the area boundaries. The distribution of spin components is effected by the area boundary as shown in Fig. 3. At first, the contour lines of iso-phase stretch out radially from the vortex core. But after dynamical evolution, they tend to meet perpendicularly with the area boundary due to the equilibrium condition $\delta H / \delta \phi \sim 0$ or $\nabla^2 \phi \sim 0$. If the lattice size is not sufficiently large, the distribution of spin components near the vortex core is effected by the area boundary. For the spin system with distance-dependent interactions, the size of the vortex core increases, so that the larger lattice size is necessary for simulations. Note also that the shape of the lattice



(a)



(b)



(c)

FIG. 3: Spin components near in-plane and out-of-plane vortex formed in the easy-plane Heisenberg model with Gaussian-type interactions. (a) The Initial state with an in-plane vortex at the lattice center with small random fluctuations of $|S_z| < 10^{-6}$ and the states after evolution for (b) $\lambda = 0.72$ and (c) $\lambda = 0.74$ ($\lambda = \varepsilon_z / \varepsilon_{xy}$, $\sigma_{xy} = \sigma_z = 1$, square lattice type and 50×50 lattice size). In-plane spin components are represented by contour lines where $\phi_i = n\pi/8$ for $n = 0, 1 \dots 15$.

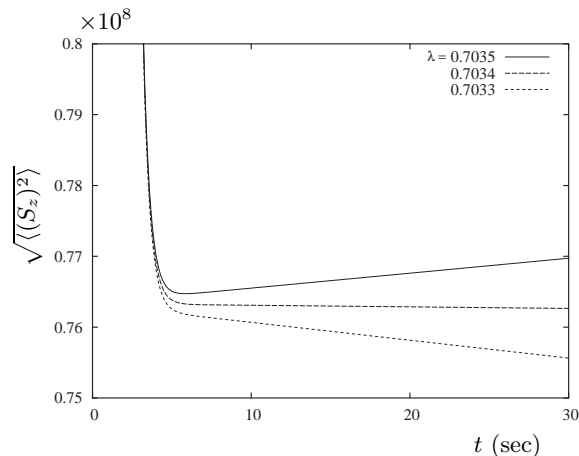


FIG. 4: The growth or decay of the S_z component in time for the CTDAHM in the case of single vortex simulation for the square lattice type (50×50 lattice size and time step of 0.001).

is matter more than its size. Note that the single vortex is attracted to the area boundary like an electric charge near the conductor surface. If there is an asymmetry in the lattice, the centered vortex may move along a certain direction. An asymmetry in the shape of the cutoff range can also induce the wandering of the vortex core. Especially the single-vortex simulations for the triangular lattice turned out to be more difficult and sensitive to the shape of the lattice and the cutoff range.

We measure the growth of the out-of-plane components by $\sqrt{\langle (S_z)^2 \rangle}$. The measurement of the squared component $(S_z)^2$ at the central peak can be another choice. However, tracing single or few components may fail to determine the vortex stability since the vortex core may start to move. In case that the vortex wanders, the fluctuations can be measured by $\sqrt{\langle (S_z)^2 \rangle}$. To clarify the simulation results, we confirm the monotonical increase or decrease after the inflection point.

Our simulational method is very fast, yielding the computed critical anisotropy that is more accurate than those by previous approaches. For example, Fig. 4 shows the results of dynamical evolution with the CTDAHM for the square lattice. We find a monotonical growth (or decay) of out-of-plane components after some time for $\lambda = 0.7035$ (or $\lambda = 0.7034, 0.7033$). This graph suggests that the critical anisotropy lies between $0.7034 < \lambda_c \leq 0.7035$, which agrees well with analytic calculations by Wysin in Ref. 9 ($\lambda_c \approx 0.703409$) and ours in Sec.III ($\lambda_c \approx 0.703420$). Similarly, we obtain $\lambda_c \approx 0.6129$ for the triangular lattice and $\lambda_c \approx 0.8330$ for the hexagonal lattice, which also agree well with the results of Wysin ($\lambda_c \approx 0.612856$ and 0.832956 respectively¹¹).

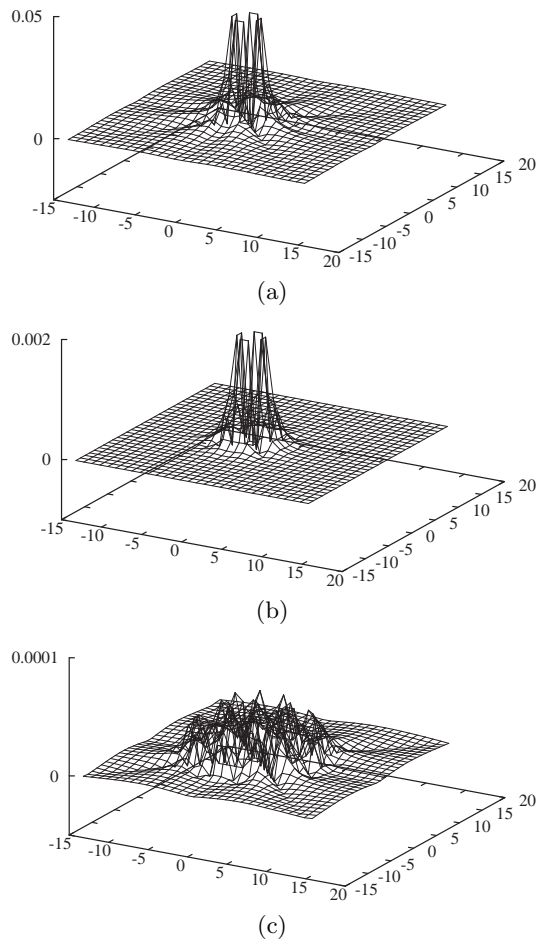


FIG. 5: Deviation in the discrete solution from the continuum result near the vortex core for the square lattice, where the x - and y -axis are the lattice coordinates and the z -axis denotes $|\sin(\phi_{dis} - \phi_{cont})|$ for (a) the nearest-neighbor interactions (b) the Gaussian type interactions with $\sigma_{xy} = 1$ and (c) the Gaussian type interactions with $\sigma_{xy} = 4$.

V. EXPERIMENTS IN GAUSSIAN TYPE INTERACTIONS

As a typical example of the spin systems with an arbitrary distance-dependent interaction types, we study the model with Gaussian type interactions where

$$I_\mu(r) = \exp(-r^2/2\sigma_\mu^2). \quad (5.1)$$

In the continuum limit, the fourier transformed interaction,

$$\tilde{I}_\mu(q) = \pi \left(\frac{\sigma_\mu}{a} \right)^2 \exp(-\sigma_\mu^2 q^2/2), \quad (5.2)$$

has a maximum at $q = 0$ and the approximated Hamiltonian can be written as Eq.(2.5) with $J_s = \pi \varepsilon_{xy} \sigma_{xy}^2 / a^2$, $\delta = 1 - (\varepsilon_z / \varepsilon_{xy})(\sigma_z^2 / \sigma_{xy}^2)$, $\delta' = 1 - (\varepsilon_z / \varepsilon_{xy})(\sigma_z^4 / \sigma_{xy}^4)$, $\alpha^2 = 2\sigma_{xy}^2$ and the anisotropy

$$\lambda = \frac{\varepsilon_z \sigma_z^2}{\varepsilon_{xy} \sigma_{xy}^2}. \quad (5.3)$$

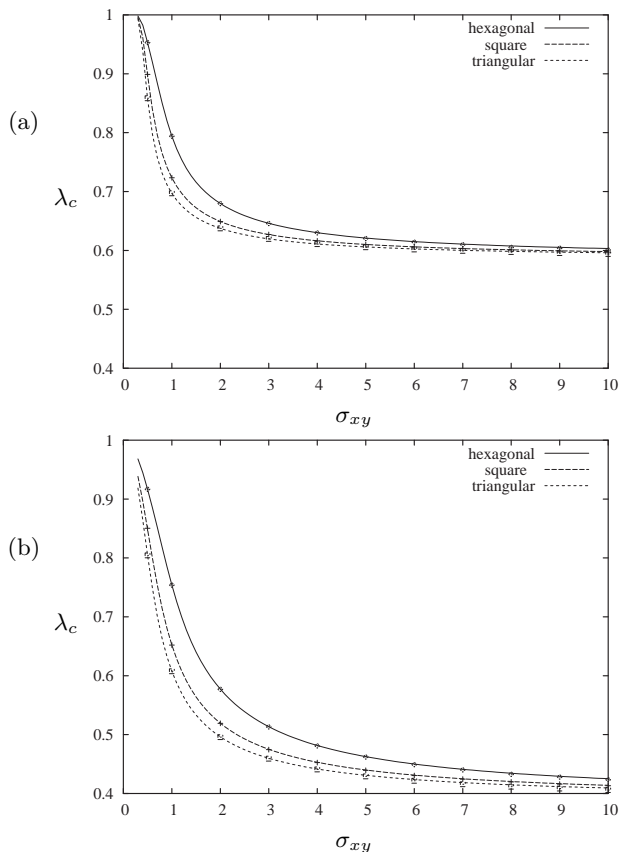


FIG. 6: The critical anisotropy λ_c as a function of σ_{xy} in the anisotropic Heisenberg model with Gaussian type interactions for (a) $\lambda = \varepsilon_z/\varepsilon_{xy}$ ($\sigma_{xy} = \sigma_z$) and (b) $\lambda = \sigma_z^2/\sigma_{xy}^2$ ($\varepsilon_{xy} = \varepsilon_z$). The critical anisotropy λ_c are determined by the determinant of the 1024×1024 matrix. The symbols denote the results of the numerical simulations.

The critical anisotropy λ_c is not uniform but varies depending on ε_μ and σ_μ . We can investigate the behaviour of the critical anisotropy from Gaussian type interactions for two different general cases; the exchange strengths are proportional to each other, $J_z(r)/J_{xy}(r) = \text{const}$ for all r or $\lambda = \varepsilon_z/\varepsilon_{xy}$, and the exchange energy are proportional to σ_μ^2 for the interaction range σ_μ in the two-dimensional system or $\lambda = \sigma_z^2/\sigma_{xy}^2$.

In analytic calculations, a large number of the nearest components, \mathcal{N} , is needed for the convergence of the critical value λ_c as shown in Fig. 2. The critical values of the anisotropy are determined for $\mathcal{N} = 1024$. For the case of $\lambda = \varepsilon_z/\varepsilon_{xy}$, the critical anisotropy is found by the condition that the determinant of the $\mathcal{N} \times \mathcal{N}$ matrix, W , vanishes where

$$W_{\alpha\beta} = \delta_{\alpha\beta} \sum_{i \in M_\alpha} \sum_j \exp(-r_{ij}^2/2\sigma_{xy}^2) \cos(\phi_i - \phi_j) - \lambda \sum_{i \in M_\alpha} \sum_{j \in M_\beta} \exp(-r_{ij}^2/2\sigma_{xy}^2). \quad (5.4)$$

The maximal eigenvalue λ of Eq.(5.4) gives the critical anisotropy λ_c as in Eq.(3.5). The angles of in-plane com-

TABLE I: Linear fitting of $\sigma_{xy}\sqrt{\lambda_c}$ as a function of σ_{xy}

Lattice type	$\lambda = \varepsilon_z/\varepsilon_{xy}$		$\lambda = \sigma_z^2/\sigma_{xy}^2$	
	slope	y-intercept	slope	y-intercept
Square	0.764928	0.082300	0.625910	0.181816
Hexagonal	0.765017	0.116011	0.629297	0.243578
Triangular	0.764967	0.068548	0.624828	0.154744

ponents ϕ_i are initially set to their continuum vortex values, $\phi_i = \tan^{-1}(y_i/x_i)$, for each site i and evolved until they approach the equilibrium state according to the dynamical equation,

$$\frac{\partial \phi_i}{\partial t} = -2 \sum_j J_{xy}(r_{ij}) \sin(\phi_i - \phi_j) \quad (5.5)$$

from Eq.(4.1a) with $m_i = 0$ for all sites, that is, the discrete dynamics in the absence of out-of-components or the pure XY model limit. Note that the spin configuration of the system with distance interaction, however, corresponds well to the continuum results near the vortex core in contrast to one with the nearest-neighbor interaction. There are much differences between our results and the classical models with the nearest-neighbor interactions, which decreases as the interaction range increases for the Gaussian type interactions. Fig. 5 shows the differences between the discrete solutions and the continuum solutions. The discrete solutions are obtained after the evolution from the continuum solution $\phi_i = \tan^{-1}(y_i/x_i)$ by Eq.(5.5), avoiding the area boundary effect by using a round shaped lattice boundary ($R = 80$). However, we solve the equations with the initial angles or setting $\cos(\phi_i - \phi_j) = \hat{r}_i \cdot \hat{r}_j$ for Gaussian type interactions, and which leads to the accurate results. For $\lambda = \sigma_z^2/\sigma_{xy}^2$, the matrix W is given by

$$W_{\alpha\beta} = \delta_{\alpha\beta} \sum_{i \in M_\alpha} \sum_j \exp(-r_{ij}^2/2\sigma_{xy}^2) \cos(\phi_i - \phi_j) - \sum_{i \in M_\alpha} \sum_{j \in M_\beta} \exp(-r_{ij}^2/2\lambda\sigma_{xy}^2), \quad (5.6)$$

which is difficult to be converted as an eigenvalue problem as before. The critical anisotropy λ_c is determined by $f(\lambda) = \det |W(\lambda)|$ in Eq.(5.6) using the root finding method, which is in agreement with the results of numerical simulations within the accuracy of two- or three-digits. We show the analytic and simulation results for square, hexagonal and triangular lattices in Fig. 6.

The obtained critical value of anisotropy decreases as the interactions range σ decreases. Note that the computed values of the critical anisotropy λ_c are in the order of hexagonal, square and triangular lattices type for both $\lambda = \varepsilon_z/\varepsilon_{xy}$ and $\lambda = \sigma_z^2/\sigma_{xy}^2$ as in the CTDAHM. Fig. 7 shows the plot of $\sigma_{xy}\sqrt{\lambda_c}$ as a function of σ_{xy} , showing a linearity between them. The slopes for different lattice types can be grouped as two classes with $\lambda = \varepsilon_z/\varepsilon_{xy}$

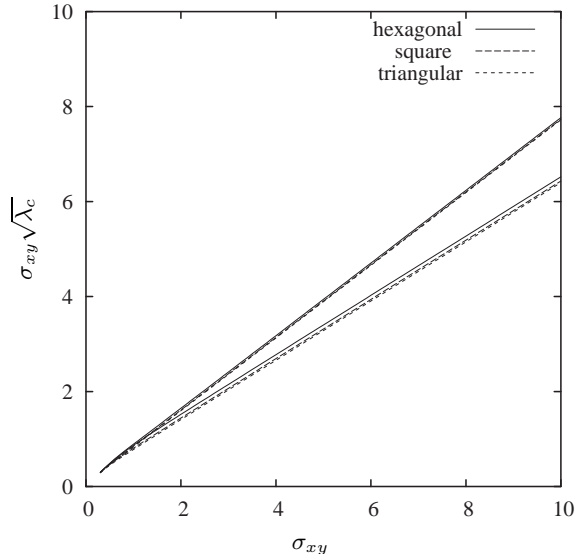


FIG. 7: $\sigma_{xy}\sqrt{\lambda_c}$ as a function of σ_{xy} . The upper branch corresponds to $\lambda = \varepsilon_z/\varepsilon_{xy}$ and lower branch to $\lambda = \sigma_z^2/\sigma_{xy}^2$. When $\lambda = \sigma_z^2/\sigma_{xy}^2$, y-axis means σ_z .

and $\lambda = \sigma_z^2/\sigma_{xy}^2$ (Table I). If the linearity is maintained for all σ_{xy} , the asymptotic value of $\sqrt{\lambda_c}$ will converge to the slope of the line for large σ_{xy} . With the help of the asymptotic solutions in Eq.(5.4) and Eq.(5.6), we can guess that the critical anisotropy λ_c will converge to zero and the slope of lines in Fig. 7 will become smaller for large σ_{xy} .

When $\varepsilon_{xy} = \varepsilon_z$ and $\sigma_{xy} = \sigma_z = 1/\sqrt{2}$, the approximated Hamiltonian with Gaussian type interactions in Eq.(2.5) becomes that

$$H \simeq -NJ_s S^2 + \frac{J_s S^2}{4} \int d^2r \left\{ (1-m^2)(\nabla\phi)^2 + [1-\delta(1-m^2)] \frac{(\nabla m)^2}{(1-m^2)} + 4\delta m^2 \right\}, \quad (5.7)$$

which is equivalent to that of the CTDAHM⁵ with a coupling constant of nearest-neighbor interactions $J_s/2$. In this case, they have the common ground-state energy and the common excitation energy due to formation of a vortex for the same lattice type and lattice size. However, we find that the critical anisotropy λ_c in Gaussian type interactions is 0.7938 from analytic calculations and 0.7941 from simulational experiments for square lattice, which are different with $\lambda_c \approx 0.7035$ in the CTDAHM. These results mean that the solutions of the critical anisotropy from the continuum limit approach are inadequate.

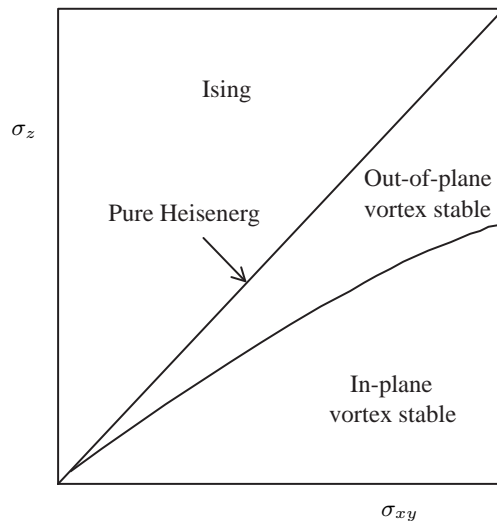


FIG. 8: Crossover behavior for interaction ranges.

VI. DISCUSSION

We have studied the vortex formation in the two-dimensional anisotropic Heisenberg model with distance-dependent interactions and determined the critical anisotropy λ_c precisely for Gaussian type interactions. The continuum theory helps to predict how spin configurations will develop for an arbitrary shaped exchange function $J_\mu(r)$. If the exchange energy function $J_\mu(r)$ satisfies certain conditions, the approximated Hamiltonian in the continuum limit has a similarity to that of the CTDAHM, which leads to the similarity in two types of static vortex solutions. However, the continuum theory breaks down in determining the critical anisotropy as noted by Wysin⁷. We also give an example that two different anisotropic Heisenberg models with a common approximated form in the continuum limit can have different critical anisotropies.

It is very difficult to determine the critical anisotropy for an arbitrary type of the exchange energy function $J_\mu(r)$. In this paper, we have studied two typical cases by using Gaussian type interaction models. One case is that $J_{xy}(r)$ and $J_z(r)$ are proportional for all r and another case is that $J_{xy}(r)$ and $J_z(r)$ have a common distribution type with different interaction ranges. The results for these cases suggest some general behaviors of λ_c . The critical anisotropy is the smallest for the triangular lattice and is the largest for the hexagonal lattice among three lattice types explored. This is also the case for the classical model because the spins near the vortex core tend to be more parallel, reducing their total exchange energy further, so that the lattice type with more nearest neighborhoods can reduce the out-of-plane exchange energy further while increasing the in-plane exchange energy for lower value of λ . Fig. 8 shows the crossover behavior of spin dynamics when the anisotropy between the in-plane and the out-of-plane energies is manifested only by the

difference in interaction ranges. If the interaction range of the in-plane is larger than that of the out-of-plane ($\sigma_{xy} > \sigma_z$), the number of exchange pairs in the in-plane case is larger for the ferromagnetic system and the system belong to the same universality class as the XY model. The region where the out-of-plane vortex is stable can be approximately found in the region with $\alpha < \sigma_z/\sigma_{xy} < 1$, for a reasonable range of σ . If σ_{xy} is very large in comparison with the nearest-neighbor distance, a nearly zero critical anisotropy may occur.

Our study for the precise determination of the critical anisotropy is motivated from the problem of the map formation in the cerebri cortex rather than magnetism systems. The results for the crossover among the regions with Ising, stable out-of-plane or stable in-plane vortex behaviors depending on the interaction ranges in Fig. 8 correspond well with the data from the animal experiments for different types of the map formation in the visual cortex⁹.

* Electronic address: mwcho@postech.edu

† Electronic address: swan@postech.edu

¹ V. L. Berezinskii, *Teor. Fiz.* **61**, 1144 (1971).

² J. M. Kosterlitz and D. J. Thouless, *J. Phys. C* **6**, 1181 (1973).

³ J. M. Kosterlitz, *J. Phys. C* **7**, 1046 (1974).

⁴ G. M. Wysin, M. E. Gouvêa, A. R. Bishop, and F. G. Mertens, in *Computer Simulations Studies in Condensed Matter Physics*, edited by D. P. Landau, K. K. Mon, and H.-B. Schütter (Springer-Verlag, Berlin, 1988).

⁵ M. E. Gouvêa, G. M. Wysin, and A. R. Bishop, *Phys. Rev. B* **39**, 11840 (1989).

⁶ J. E. R. Costa and B. V. Costa, *Phys. Rev. B* **54**, 994 (1996).

⁷ G. M. Wysin, *Phys. Rev. B* **49**, 8780 (1994).

⁸ M. W. Cho and S. Kim, *Phys. Rev. Lett.* (to be published) (2003), arXiv:Physics/0306047.

⁹ M. W. Cho and S. Kim, *Different ocular dominance map formation influenced by orientation preference columns* (2003), arXiv:q-bio.NC/0310039.

¹⁰ S. Takeno and S. Homma, *Theor. Phys.* **64**, 1193 (1980).

¹¹ G. M. Wysin, *Phys. Lett. A* **23**, 96 (1998).